EXPERIMENTAL VERIFICATION OF ABS CONCRETE DESIGN METHODOLOGY APPLIED TO THE DESIGN OF THE FIRST COMMERCIAL SCALE FLOATING OFFSHORE WIND TURBINE IN THE UNITED STATES

Mark G. Dwyer
University of Maine
Orono, ME, USA

Anthony M. Viselli
University of Maine
Orono, ME, USA

Habib J. Dagher
University of Maine
Orono, ME, USA

Andrew J. Goupee
University of Maine
Orono, ME, USA

ABSTRACT

The abundance of consistent high strength winds off the world's coastlines and the close proximity to dense population centers has led to development of innovative marine structures to support wind turbines to capture this energy resource. Off the US coast, 60% of the offshore wind lies in deep water (greater than 60m) where the development of Floating Offshore Wind Turbine (FOWT) hull technology will likely be required in lieu of fixed bottom technology such as jacket structures. The United States National Renewable Energy Laboratory (NREL) and the offshore wind community commonly refer to 60m as the transition point between fixed bottom structures and floating structures due to economic reasons. Floating wind turbines deployed in the harsh offshore marine environment require the use of materials that are cost-effective, corrosion resistant, require little maintenance and are highly durable. This has led the University of Maine to develop a concrete hull technology called VolturnUS for full-scale 6MW FOWTs. In this work, experimental testing was conducted to verify the performance of the concrete under operational, serviceability, and extreme loading conditions as required by the *American Bureau of Shipping Guide for Building and Classing Floating Offshore Wind Turbines*. The testing included structural testing sub-components of the hull and served as experimental verification of American Bureau of Shipping (ABS) concrete design methodology which is currently approved and being used to design the first commercial scale FOWTs in the United States. Two 6MW wind turbines supported on VolturnUS concrete hulls will be used for the New England Aqua Ventus I project. The project is planned to be deployed and connected to the grid by 2019 in the Northeast U.S. and is funded by the US Department of Energy.

INTRODUCTION

This paper presents results from an experimental structural testing program aimed to verify the American Bureau of Shipping (ABS) concrete design methodology for floating offshore wind turbines (FOWT). The test data was used as part of the design of the first commercial scale floating concrete hull supporting an offshore wind turbine in the United States. The University of Maine is currently designing a floating concrete semi-submersible hull for a full-scale 6MW FOWT using a hull technology called VolturnUS [1-6].

An overview of the use of concrete for floating structures is now presented. In recent years, a significant interest has developed in the use of FOWT. These installations offer several advantages over land-based and fixed-bottom wind turbine installations including access to more abundant and steady wind resources, reductions in view-shed issues, and close proximity to dense population centers. The United States National Renewable Energy Laboratory (NREL) inventory of available renewable energy resources within the U.S. shows that winds off the U.S. coastline over water depths of 100ft (30m) have the energy capacity of 3,200TWh/yr, equivalent to approximately 85% of the total U.S. energy use of 3,740 TWh/year [7]. As a result, many groups are now researching floating wind turbine systems to capture this deep water resource. Floating turbine platform technology concepts to date have employed similar design concepts as the offshore oil and gas sector including tension leg platforms, semi-submersibles, and spar buoys.

For offshore wind turbines, the levelized cost of energy (LCOE) is the critical driver to meet the US Department of Energy's goal of 20% U.S. wind energy use by 2030 [8]. This has led the University of Maine to investigate optimized

configurations for FOWTs to reduce cost and increase power production. Concrete can offer cost-effectiveness, increased durability, and utilize local labor resources to construct prestressed/post-tensioned concrete for the hull structure. Concrete is typically more durable than steel in an offshore environment with little or no maintenance as compared to the traditional 20-year life cycle steel approach [9].

The offshore oil and gas industry has taken advantage of floating concrete structures. Several large offshore oil & gas floating concrete platforms are deployed today including the Troll B semi-submersible and the Heidrun TLP located in the North Sea. The Troll B semi-submersible platform has a total weight of 125,500 MT and was built with four rectangular pontoons [10]. The Heidrun TLP, shown in Figure 1, carries over 43,200 MT of topside, has a hull mass of 288,200 MT, was deployed in the 1990's, and continues to produce to this day with little to no maintenance of the concrete hull [11]. Offshore concrete structures are typically designed to have a 50-70 year service life. This is achieved by the use of well compacted low permeability concrete that protects the concrete and reinforcement. Concrete, when submerged in water also continues to gain strength and heals damage [12].

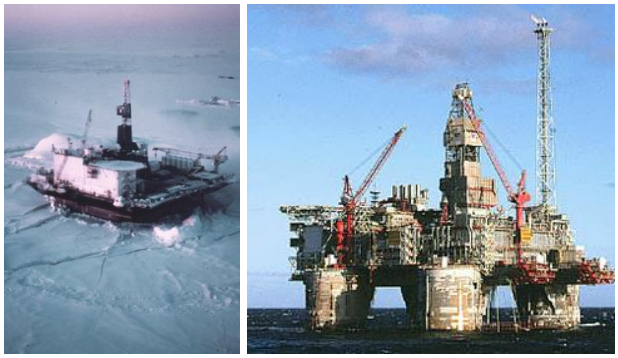

FIGURE 1. CIDS CONCRETE PLATFORM [13] (LEFT) AND HEIDRUN TLP OPERATED BY STATOIL HYDRO (RIGHT)[1]

Similar durability has been seen in concrete ships. Concrete ships constructed during World War II with lower strength conventional concrete have shown excellent durability for several decades [14]. The SS Selma vessel fabricated even earlier in 1919 began its life with a concrete compressive strength of 5,000 psi (34MPa). In 1953, small core samples were removed and the strength was found to be 8,000 psi (55MPa) and in 1980 core samples showed strength of 16,000 psi (110MPa). The concrete continually grew stronger due to access to water throughout its life.

Concrete has proven so durable in bridge construction (typical design life is 75 to 100 years) and offshore oil and gas platforms, that it can offer the potential for significantly increased service life. This is in contrast to the single 20-year life assumed for conventional steel offshore wind installations. Such an effort has already been implemented for several oil and gas platforms. For example, the Concrete Island Drilling Station (CIDS), shown in Figure 1, was originally constructed in 1984 for deployment in Alaska. This very extreme environment required the concrete to withstand 900 psi (6.2 MPa) ice pressures. In 2001, after 17 years of service, Exxon purchased the platform, refurnished it, and redeployed it off the coast of Northern Russia. The unit continues to operate today with minimal repairs or maintenance to the concrete structure [13].

In addition to the durability advantages over steel, concrete has great potential for local fabrication. Steel fabrication requires specialized labor and equipment available only at limited facilities located is a few geographic locations; primarily along the Gulf of Mexico in the U.S., Finland and Southeast Asia. This leaves many regions of the world at a loss to use local labor to build floating offshore wind hulls. An example is the New England region of the U.S. New England has high electricity demand and prices, and excellent offshore wind resources [8]. However, New England has limited cost-effective heavy steel fabrication capabilities, but does have significant experience constructing concrete for heavy bridge infrastructure which can be constructed with local labor and materials. These benefits have been realized in the bridge industry with numerous bridges such as the Raymond E. Baldwin Bridge [15] or the Penobscot Narrows Bridge shown in Figure 2. This approach could be applied to offshore wind turbines in this region. The use of local labor and facilities has also been realized in Norway where many offshore concrete platforms (mostly fixed bottom gravity structures) have been constructed and deployed in the North Sea. Over 90% of their hulls are constructed locally [12]. Concrete construction requires large amounts of unskilled labor that can be easily mobilized and could be a main driver for acceptance of offshore wind and industrialization in these regions.

FIGURE 2. CONCRETE PENOBSCOT NARROWS BRIDGE[2]

Floating concrete wind turbine hulls for a large commercial scale farm (500MW to 1000MW) are at a much larger scale than that of the above noted concrete projects. To date no floating concrete hulls supporting a wind turbine have been approved and classified by ABS. To derisk the structural design of the University of Maine project, assumptions for fatigue,

[1] http://www.tu.no/artikler/statoilhydro-far-hms-refs/322092

[2] www.snowpondphoto.com

serviceability, and strength design limit states developed for the VolturnUS 6MW design effort and presented in the current applicable guides released by ABS were verified through experimental testing. The two guides are the *Guide for Building and Classing Floating Offshore Wind Turbines* and *Guide for Building* and *Classing Fixed-bottom Offshore Wind Turbines*. A review of technical literature on submerged concrete including flexural fatigue of plain concrete, flexural fatigue of prestressed concrete, water-tightness and serviceability were found and used to guide the testing program presented in this paper [16-20].

The following sections of this paper present testing results for concrete design details adapted for a concrete offshore floating wind turbine hull. This work consists of flexural, fatigue, and water-tightness testing. The testing focused on concrete subjected to bending loads and external water pressure.

VOLTURNUS 6MW CONCRETE FLOATING WIND TURBINE HULL OVERVIEW AND CONCRETE DESIGN DETAILS TESTED

VolturnUS is a new floating wind turbine concrete hull technology developed by the University of Maine. The design incorporates innovations in materials, construction, and deployment including a concrete semi-submersible hull to reduce the costs of offshore wind including: (1) The VolturnUS concrete semi-submersible floating foundation design represents a paradigm shift in offshore construction practices for offshore wind necessary to get costs down. The hull primarily consists of corrosion-resistant, fatigue-resistant, concrete utilizing onshore construction. (2) The entire system can be completely assembled quayside with availability of only 10m of water depth. The VolturnUS can be towed out with low-cost tug boats from a number of assembly locations. (3) The VolturnUS can be anchored in multiple ways depending on site conditions, such as relatively inexpensive drag anchors in areas of sufficient sediment depth. (4) The 10m VolturnUS transit draft allows for towing the unit back to shore if major operations and maintenance activities are required. A 1:8-scale prototype was designed, constructed, and deployed in 2013. The unit was the first grid-connected offshore wind turbine in the Americas (Figure 3). It was a 1:8-scale prototype based on a full-scale 6MW unit situated farther offshore in the Gulf of Maine [2,5,21,22]. The 1:8-scale testing was performed to derisk the VolturnUS 6MW technology, however, certain concrete details are required in a full-scale design that were not demonstrated in the VolturnUS 1:8. As such, there is a need to derisk the underwater concrete details of a full-scale VolturnUS through laboratory testing.

EXPERIMENTAL TEST PROGRAM

An experimental structural testing program was developed to characterize the performance of water-tight concrete structural systems for construction of the 6MW VotlurnUS hull. The *ABS Guide for Building and Classing Gravity-based Offshore LNG Terminals* [23] provides guidance for the design of offshore concrete structures for fatigue and serviceability guidelines. These guidelines include water-tightness requirements. To ensure that the particular concrete mix and design details proposed for the VolturnUS hull do in fact meet the design limits specified by ABS, a four-point-bending test with a span of 86 in. (2,184 mm) of a typical scaled wall section including all construction details was conducted. Figure 4 shows a bending test specimen.

FIGURE 3. (LEFT) VOLTURNUS 6MW FULL-SCALE DESIGN AND (RIGHT) 1:8 PROTOTYPE DEPLOYED IN JUNE, 2013

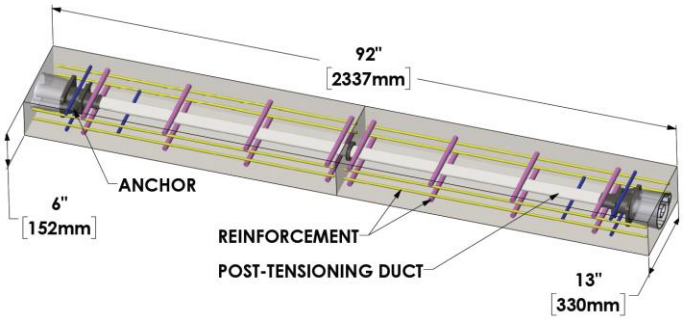

FIGURE 4. MODEL OF TEST BEAM

Test specimens were fabricated utilizing a custom offshore concrete mix developed for the VolturnUS hull containing rebar and a commercially available post-tensioning system with 2-0.5 in. (12.7 mm) 7-wire strands to subject the section to comparable post-tensioning levels as the full-scale structure. The test beams were 6 in. (152 mm) thick by 13 in. (330 mm) wide and 92 in. (2,337 mm) long with a test span of 86 in. (2,184 mm). The size was chosen to represent the details found on the full scale 6MW VolturnUS unit but remain small enough to be tested with available test equipment. The post-tensioning anchors were poured back and sealed with grout similar to full-scale construction. The jacking force on the two post-tensioning strands was 66 kips (294 kN) putting a stress of 846 psi (5.83 MPa) on the beam cross section. All losses including post-tensioning anchorage seating, elastic shortening of concrete, steel stress relaxation, concrete creep, and concrete shrinkage

were considered. Losses were calculated following ACI-318-14 [24] and account for the properties of the steel, concrete, and environmental conditions including heat, humidity, concrete curing procedure, and duration experienced by the test specimens prior to testing. For these specimens, the effects of immersion in saltwater on the losses were not included. The focus of this study was not to quantify losses but rather to confirm structural design models for serviceability, fatigue, and strength. The calculated force on the section at the start of testing, accounting for all losses, was 30.6 kips (136 kN), producing a stress of 392 psi (2.70 MPa) on the beam cross section. A drawing of the specimen and test setup is shown in Figure 5 and the operating test setup is shown in Figure 6(a). The beam was tested in a four-point bending configuration. The load was applied at two points, each 10 in. (254 mm) off center.

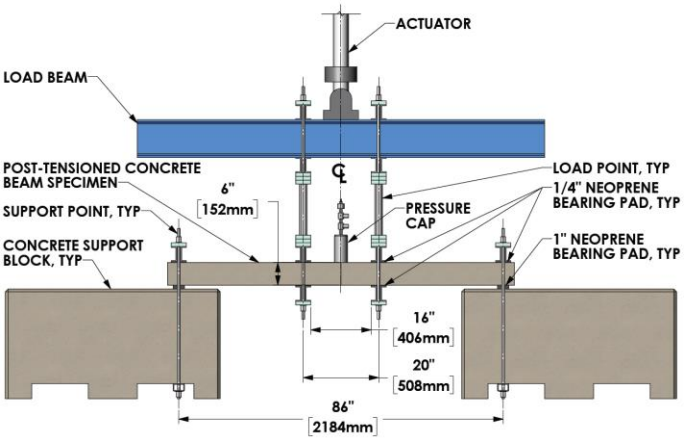

FIGURE 5. SIDE ELEVATION OF TEST SETUP

To study the water-tightness of the concrete, a method of subjecting the concrete to equivalent extreme water pressure was devised. A steel pressure cap was adhered at the centerline of one side of the concrete specimen leaving the space under the cap free for water contact (Figure 6(b)). The objective of bonding a pressurized cap to the surface of the concrete beam specimen was to identify cracks in the concrete which would lead to leakage as identified by a pressure drop. To the authors' knowledge, no standardized method exists for testing water tightness of concrete at high hydrostatic/dynamic pressures. To verify that a pressure drop is in fact due to a crack in the concrete specimen, a verification effort was conducted. Unloaded and un-cracked concrete specimens, measuring 14 in. (356 mm) by 14 in. (356 mm) by 4 in. (102 mm) thick were fabricated and the pressurized cap was installed and pressurized to the specified pressure. The cap maintained the specified pressure for a duration of time equal to that of the structural testing. With this verification effort complete, it was assumed that a pressure drop in cap on a structurally loaded specimen would in fact be due to a crack in the concrete under the cap.

The cap was filled 2/3 full of water and pressurized with air to 53.3 psi (0.37 MPa), the equivalent of 120 feet (36.6 m) of head pressure. This is the maximum static plus dynamic water pressure expected for the VolturnUS hull. Pressure data was collected from the cap during failure bending tests using a pressure gage. A second pressure cap was adhered to an unloaded control block of concrete for comparison. The cap was adhered to the compression face of the beam. The cap was applied to the region undergoing maximum compressive stress.

(a) (b)

FIGURE 6. (A) FOUR-POINT BENDING TESTING SET-UP (B) PRESSURE CAP

Instrumentation for stiffness checks and failure loading consisted of two string pots attached at mid-span on either side of the beam to record deflection. The string pots were attached to a yoke mounted to the beam to remove deflection errors due to neoprene support padding compression. Load was recorded from a load cell located in the actuator. Electronic pressure sensors recorded pressure data for the two pressure caps.

The following tests were completed using this set-up:

- **Ultimate Bending Strength Test of Post-tensioned Concrete Specimens**: A quasi-static bending test was performed on three beam specimens to failure referred to as an "Ultimate Strength Test". A pressure cap was applied to the concrete on the compression face to monitor water-tightness of the concrete during the loading process.

- **Fatigue Bending Testing Batch A of Post-tensioned Concrete Specimens:** A one-direction fatigue bending test of 43,200 cycles was performed prior to the beam being loaded to failure. Three beam specimens were tested. Beam stiffness was compared before and after the fatigue loading. A pressure cap was applied to the concrete to monitor water-tightness of the concrete after fatigue loading and during the failure loading process.

- **Fatigue Bending Testing Batch B of Post-tensioned Concrete Specimens:** A reverse loading, 2.0 x 10^6 cycle fatigue test followed by taking the beam to failure was performed on three beam specimens. Concrete is allowed to crack on one side and reach 200psi on the other face for each cycle. Beam stiffness was compared before, mid-cycle and after the fatigue

loading. A pressure cap was applied to the concrete to monitor water-tightness of the concrete during the failure loading process.

RESULTS AND DISCUSSION

Results for the quasi-static ultimate strength failure test and two fatigue tests are now presented.

Ultimate Bending Strength Test of Post-tensioned Concrete Specimens

Figure 8, Figure 9, and Figure 10 present test results for the ultimate strength of three test beams. Each figure presents the following data:

1. Measured applied load and specimen deflection at mid-span.
2. The estimated cracking load of the concrete specimen per ACI [24].
3. The measured pressure in the cap.
4. The measured pressure in the cap on an unloaded control specimen.
5. The cap installation load. This is the load point when the pressure cap was bonded to the specimen.
6. The cap release load. This is the load point where the cap detached from the specimen. This does not indicate leakage. The cap was originally bonded on at the beginning of the test but it was found that the cap would often detach due to the loads applied. The concrete was unharmed. As a result in later tests, the cap was bonded at a load close to the design ABS Serviceability Load.
7. The ABS design serviceability load for which the concrete is to be considered water-tight. For concrete design, the applied loads cannot exceed this level if the structure is to be water-tight per ABS. ABS specifies that the compression zone of the concrete in bending not be less than 25% of the thickness of the wall under un-factored extreme loads [23] to remain water-tight. This load was determined experimentally with the following method:
    - The specimen was loaded until the specimen started to crack on one side.
    - Cracks were monitored as the load increased until the cracks reached 75% of the thickness (4.5 in. (114 mm)) from the tension face as shown in Figure 7. The bending testing method produces cracks which are due to the applied tension stresses expected to be caused during extreme loading cases. The cracks do not run through the entire depth of the beam and therefore do not allow water to penetrate the hull. Concrete for other applications such as civil infrastructure is commonly designed to crack under extreme loading [24].
    - This process was repeated for four separate specimens and found to be 11,800 lbf (52.5 kN), 10,800 lbf (48.0 kN), 10,300 lbf (45.8 kN) and 9,000 lbf (40.0 kN). The average of these four measurements, 10,475 lbf (46.6 kN) was taken as the serviceability design load and used to evaluate the water-tightness of the concrete in the tests.
    - An ABS serviceability load limit of 10,475 lbf (46.6 kN) is noted on all nine test figures.

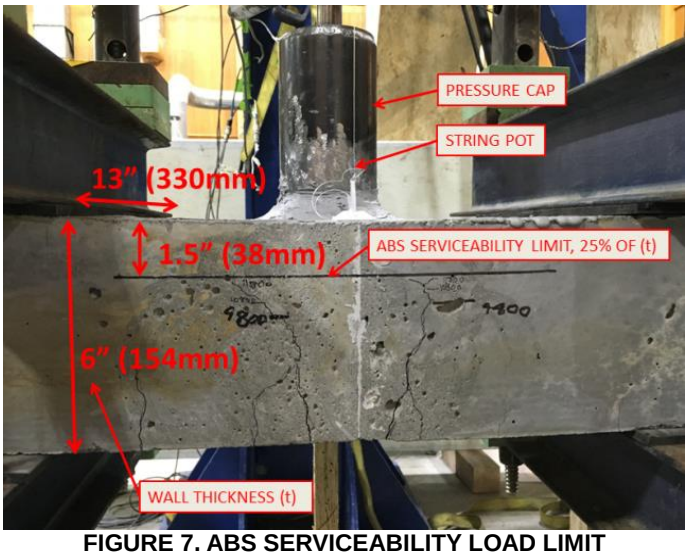

FIGURE 7. ABS SERVICEABILITY LOAD LIMIT

Specimen Ultimate Strength #1 (Figure 8) had the pressure cap adhered at the start and detached from the sample at 7,800 lbf (34.7 kN) of applied load to the beam. The maximum load was 12,290 lbf (54.7 kN). The steel cap detached due to high loads on the concrete bonding the cap to the specimen. The concrete appeared unharmed. The ACI-predicted cracking load appears to determine fairly well the actual point of cracking as indicated by the change in stiffness on Figure 8, Figure 9 and Figure 10.

To investigate the water-tightness of the concrete up to and beyond the ABS serviceability load, the Ultimate Strength #2 (Figure 9) specimen was loaded to 10,000 lbf (44.5 kN) before bonding the cap. The cap released slightly shy of the maximum load at 12,000 lbf (53.4 kN) with a maximum load of 12,322 lbf (54.8 kN). The concrete maintained water-tightness beyond the ABS serviceability load.

The pressure cap was also bonded at 10,000 lbf (44.5 kN) for the Ultimate Strength #3 (Figure 10) specimen. For this test the cap remained bonded and held pressure up to the maximum load of 13,463 lbf (59.9 kN). This demonstrates that the concrete maintained water-tightness beyond the ABS

serviceability load and even remained water-tight up to failure of the concrete by crushing.

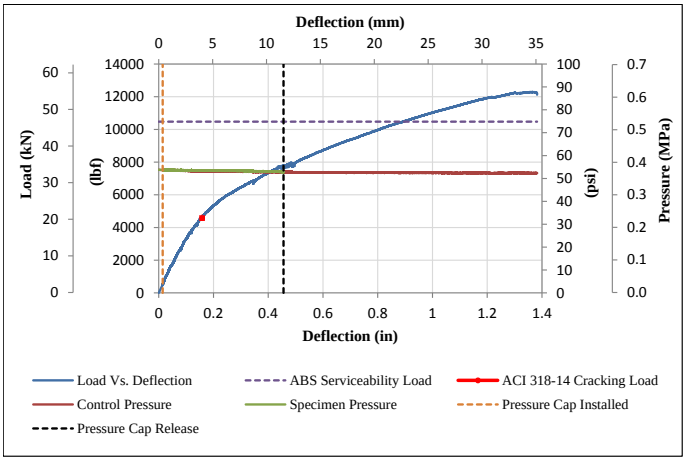

FIGURE 8. LOAD VS. DEFLECTION PLOT FOR ULTIMATE STRENGTH TEST #1, MAXIMUM LOAD 12,290 LBF

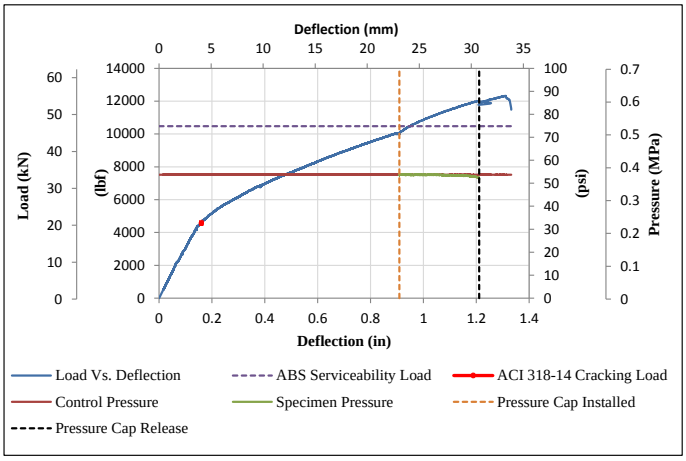

FIGURE 9. ULTIMATE STRENGTH TEST #2, MAXIMUM LOAD 12,322 LBF

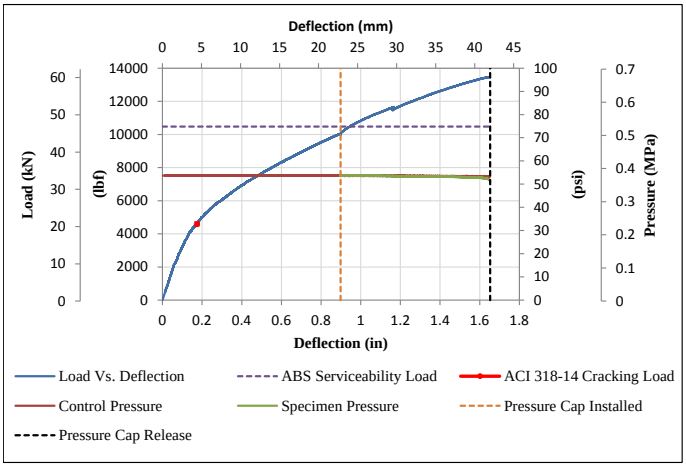

FIGURE 10. ULTIMATE STRENGTH TEST #3, MAXIMUM LOAD 13,463 LBF

Fatigue Bending Testing Batch A of Post-tensioned Concrete Specimens

Three specimens were tested to investigate the fatigue resistance, residual strength and water-tightness of the concrete when subjected to significant fatigue damage equivalent to that described in the ABS Guides. This fatigue testing consisted of applying one direction bending loading. The ABS guides specifies that when the concrete is subjected to operational/ fatigue loading, the tension stresses are not to be more than 200 psi (1.38 MPa) to be considered adequate for fatigue [23]. Stresses for the rebar are also provided but are typically not reached if the concrete is not cracked. If the concrete tension stresses exceed this limit, a more detailed fatigue analysis can be completed.

Using an S-N curve model for plain concrete, the number of cycles to failure for the concrete with 200 psi applied stress on the tensile face was estimated to be 145 x 10^6 cycles. Equation (1) is the model for the S-N curve where S is the stress level (f_{max}/MOR), R is the stress ratio (f_{min}/f_{max}), f_{max} is the maximum fatigue stress, f_{min} is the minimum fatigue stress, MOR is the modulus of rupture of the concrete, N is the number of cycles to fatigue failure and c_1 is a coefficient [16,17]. This number of cycles is not likely to be exceeded in service for an offshore wind turbine deployed for 60 years. For example, a simplistic and very conservative estimate for the number of cycles uses the mean wave period of 9 seconds, which results in 21 million cycles over a 60 year deployment.

$$S = 1 - c_1(1 - R)\log_{10} N \quad (1)$$

This cycle count is not feasible for lab testing. Therefore an equivalent higher damage loading was needed to simulate the 200 psi (1.38 MPa) of fatigue damage causing tensile failure in the concrete at a quicker rate. To evaluate the ability of the concrete to maintain water-tightness and structural capacity up to and exceeding the concrete fatigue strength, a loading regime was developed to apply enough damage to fail the concrete specimen in tension. A force of 2,956 lbf (13.1 kN) was applied 43,200 times to induce an equivalent damage using a Miner summation technique [25]. Each load cycle induced 310 psi (2.14 MPa) of tension in the concrete. This load and number of cycles produced a Miner damage summation equal to 1.0.

An initial static stiffness test was performed during the first fatigue cycle. After running the complete fatigue loading the beam was visually inspected for damage. No visible signs of damage were observed in the concrete. The initial static loading was compared to the stiffness of the specimen when taken to failure after the fatigue loading. Figure 11, Figure 12 and Figure 13 show the initial curve and final loading curve for the three beams subjected to fatigue loading then ultimate strength testing. They are referred to as Fatigue A #1 (Figure 11), Fatigue A #2 (Figure 12), Fatigue A #3 (Figure 13). The slight

discontinuities in the data are due to stoppage of the test to observe crack propagation. The average ultimate strength of the fatigue specimens showed a 6.7% decrease as compared to the uncycled specimens as shown in Table 1 and Table 2, likely indicating damage due to the fatigue loading. Table 3 and Table 4 show the change in stiffness before and after the fatigue loading. Up to an 8.5% change in stiffness was recorded indicating the concrete likely cracked due to the fatigue loading. However, the concrete maintained its water-tightness beyond the ABS serviceability load for water-tightness, and in some cases up to the ultimate strength of the beam. Fatigue A #2 and #3 specimen caps experienced some leaking due to the cap bonding process but held the majority of the applied pressure beyond the ABS serviceability load. This was not due to concrete leaking between the concrete sections.

Fatigue Bending Testing Batch B of Post-tensioned Concrete Specimens

Three other specimens were also tested to investigate the residual strength and water-tightness of the concrete when subjected to reversed bending fatigue stresses which exceed the ABS 200psi tension stress limit. This fatigue testing batch applied unbalanced reverse direction bending loading and considered the stresses in the concrete tension face and tensile stresses in the reinforcing bar. The Fatigue B cycle consisted of applying a load in the upward direction such that the top concrete fibers reached the ABS limit of 200 psi (1.38 MPa) tensile stress, followed by applying a downward load such that the concrete exceeded the 200psi (1.38 MPa) tension ABS limit. A load was applied which caused the concrete on the bottom face to crack and the bottom reinforcing steel to reach the ABS fatigue limit of 20,000 psi (137.9 MPa) of tensile stress [23]. The beam specimens were loaded 2.0 x 10^6 times following guidance from *DNV-OS-C502* [26]. DNV considers a concrete structure to be adequate for fatigue if the maximum applied fatigue load due to environmental loadings (e,g, wind, wave, and current) does not cause failure after 2.0 x 10^6 cycles.

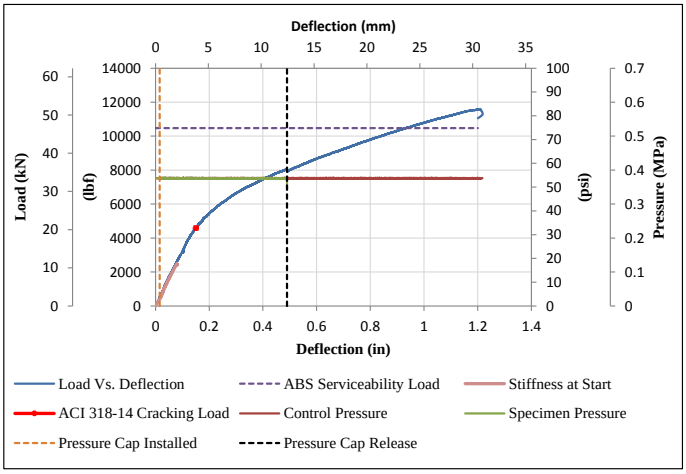

FIGURE 11. FATIGUE A #1, STIFFNESS VERIFICATION AND ULTIMATE STRENGTH TEST, MAXIMUM LOAD 11,579 LBF

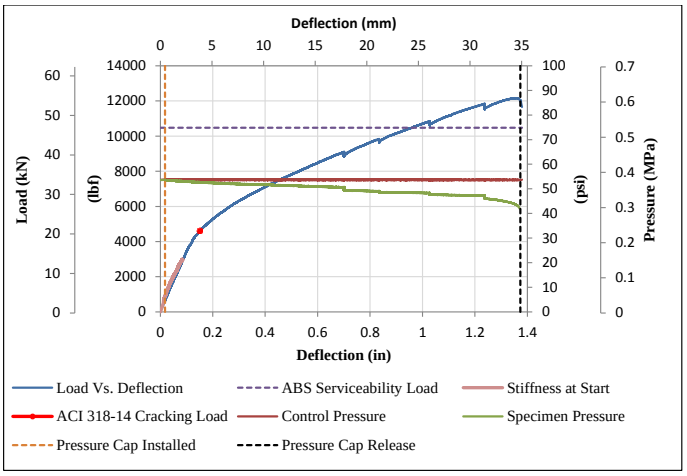

FIGURE 12. FATIGUE A #2, STIFFNESS VERIFICATION AND ULTIMATE STRENGTH TEST, MAXIMUM LOAD 12,249 LBF

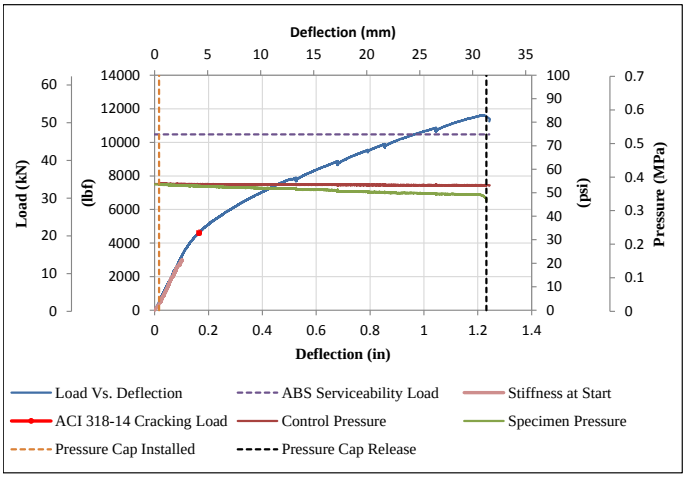

FIGURE 13. FATIGUE A #3, STIFFNESS VERIFICATION AND ULTIMATE STRENGTH TEST, MAXIMUM LOAD 11,686 LBF

TABLE 1: COMPARISON OF FAILURE LOAD FOR ULTIMATE AND FATIGUE A TESTS (IMPERIAL UNITS)

TEST TYPE	FAILURE LOAD (LBF)			MEAN	STD	COV
	TEST #1	TEST #2	TEST #3	(LBF)	(LBF)	%
ULTIMATE	12,290	12,322	13,463	12,692	668	5.3
FATIGUE A	11,579	12,249	11,686	11,838	360	3.0
			% DIFF	6.7		

TABLE 2: COMPARISON OF FAILURE LOAD FOR ULTIMATE AND FATIGUE A TESTS (METRIC UNITS)

TEST TYPE	FAILURE LOAD (kN)			MEAN	STD	COV
	TEST #1	TEST #2	TEST #3	(kN)	(kN)	%
ULTIMATE	54.67	54.81	59.88	56.45	2.97	5.3
FATIGUE A	51.50	54.48	51.98	52.66	1.60	3.0
			% DIFF	6.7		

TABLE 3: CHANGE IN BEAM STIFFNESS DUE TO FATIGUE A LOADING (IMPERIAL UNITS)

TEST	SLOPE: INITIAL (KIP/IN)	SLOPE: ULTIMATE (KIP/IN)	% DIFFERENCE
FATIGUE A #1	34.3	34.5	0.7
FATIGUE A #2	37.7	34.5	-8.5
FATIGUE A #3	34.3	31.8	-7.5

TABLE 4: CHANGE IN BEAM STIFFNESS DUE TO FATIGUE A LOADING (METRIC UNITS)

TEST	SLOPE: INITIAL (kN/mm)	SLOPE: ULTIMATE (kN/mm)	% DIFFERENCE
FATIGUE A #1	6.00	6.04	0.7
FATIGUE A #2	6.61	6.05	-8.5
FATIGUE A #3	6.01	5.56	-7.5

A quasi-static load cycle was performed to evaluate beam stiffness at 1, 1.0 x10^6 and 2.0 x 10^6 cycles. The results are shown in Figure 14, Figure 15 and Figure 16. The majority of the decrease in stiffness appears to occur during the first 1.0 x 10^6 cycles as the concrete begins to crack on the bottom face only. The load to produce the 20,000 psi (137.9 MPa) of reinforcing tensile stress is above the tensile modulus of rupture load for the concrete. Cracks are visible during the fatigue loading. Table 5 shows the percent decrease in beam stiffness from 0% to 100% of the fatigue loading. Figure 17, Figure 18 and Figure 19 show test results for the ultimate strength of the beams following the Fatigue B testing. The slight discontinuities in the data are due to stoppage of the test to observe crack propagation. The average ultimate strength of the fatigue specimens showed a 6.9% decrease as compared to the uncycled specimens as shown in Table 6 and Table 7. This is comparable to the Fatigue A decreases.

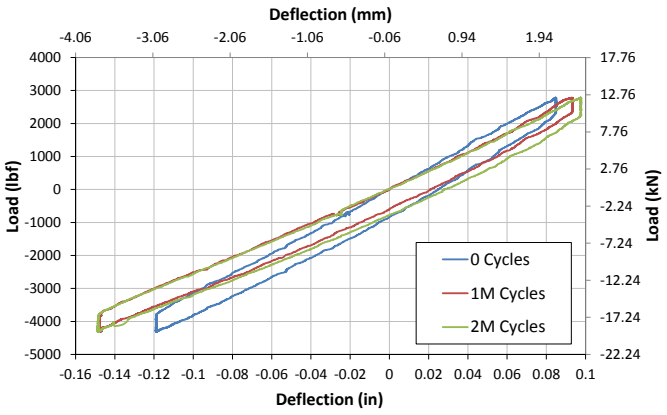

FIGURE 14. FATIGUE B #1 BEAM STIFFNESS

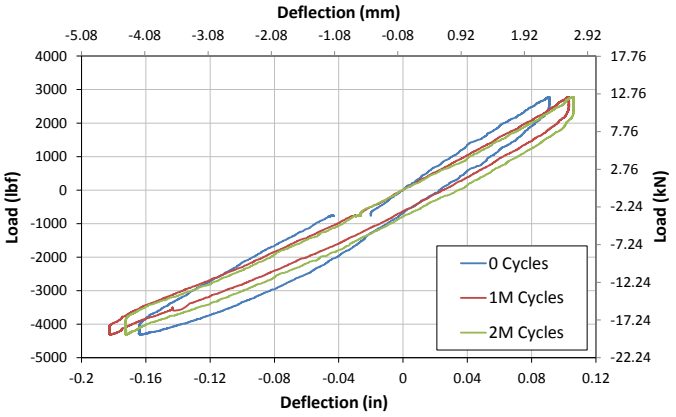

FIGURE 15. FATIGUE B #2 BEAM STIFFNESS

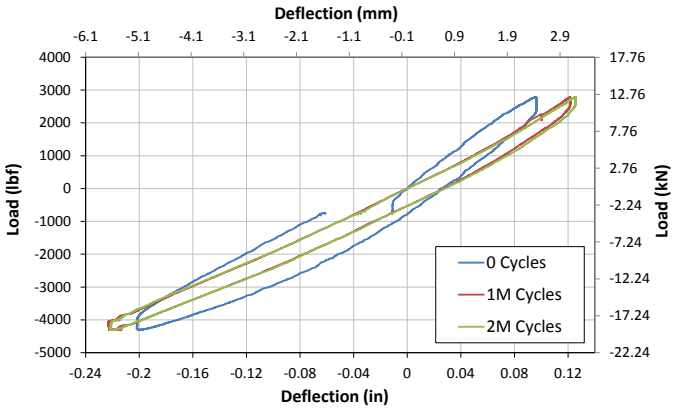

FIGURE 16. FATIGUE B #3 BEAM STIFFNESS

TABLE 5: CHANGE IN BEAM STIFFNESS DUE TO FATIGUE B LOADING

	STIFFNESS		PERCENT OF FATIGUE 0%	50%	100%	DECREASE IN STIFFNESS
FATIGUE B #1	TENSION	(KIP/IN)	33.65	29.44	28.72	-17%
		(kN/mm)	5.89	5.16	5.03	
	COMPRESSION	(KIP/IN)	29.50	23.54	22.89	-29%
		(kN/mm)	5.17	4.12	4.01	
FATIGUE B #2	TENSION	(KIP/IN)	30.16	26.08	26.36	-14%
		(kN/mm)	5.28	4.57	4.62	
	COMPRESSION	(KIP/IN)	21.67	19.42	19.88	-9%
		(kN/mm)	3.80	3.40	3.48	
FATIGUE B #3	TENSION	(KIP/IN)	30.69	23.00	22.30	-38%
		(kN/mm)	5.37	4.03	3.91	
	COMPRESSION	(KIP/IN)	17.16	16.89	16.79	-2%
		(kN/mm)	3.00	2.96	2.94	

TABLE 6: COMPARISON OF FAILURE LOAD FOR ULTIMATE AND FATIGUE B TESTS (IMPERIAL UNITS)

TEST TYPE	FAILURE LOAD (LBF) TEST #1	TEST #2	TEST #3	MEAN (LBF)	STD (LBF)	COV %
ULTIMATE	12,290	12,322	13,463	12,692	668	5.3
FATIGUE B	12,412	11,740	11,288	11,813	566	4.8
			% DIFF	6.9		

TABLE 7: COMPARISON OF FAILURE LOAD FOR ULTIMATE AND FATIGUE B TESTS (METRIC UNITS)

TEST TYPE	FAILURE LOAD (kN)			MEAN	STD	COV
	TEST #1	TEST #2	TEST #3	(kN)	(kN)	%
ULTIMATE	54.67	54.81	59.88	56.45	2.97	5.3
FATIGUE A	55.21	52.22	50.21	52.55	2.52	4.8
			% DIFF	6.9		

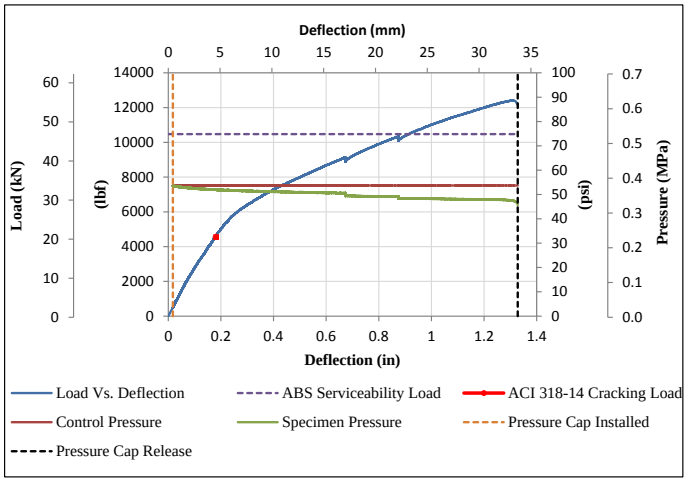

FIGURE 17. FATIGUE B #1 ULTIMATE STRENGTH TEST, MAXIMUM LOAD 12,412 LBF

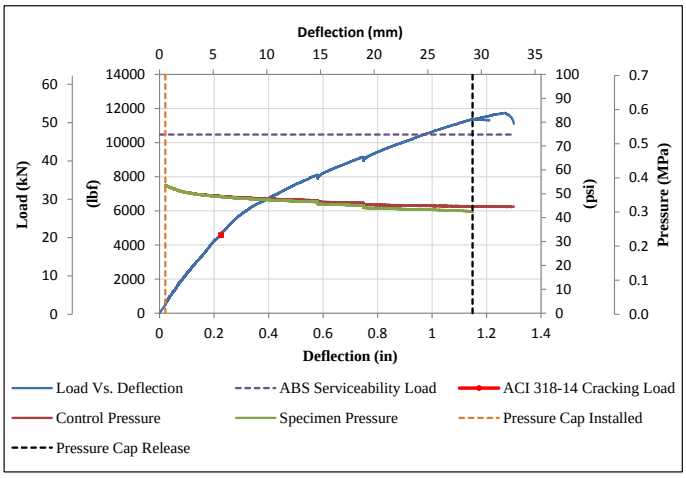

FIGURE 18. FATIGUE B #2 ULTIMATE STRENGTH TEST, MAXIMUM LOAD 11,740 LBF

CONCLUSIONS

A testing program was developed to verify that the ABS design procedures adequately predict the behavior of the VolturnUS-specific concrete mix and design details when subjected to extreme and fatigue bending loads while maintaining water-tightness. The testing focused on bending loads as these are a primary driver for concrete design. Through this effort, the concrete in all cases was found to exceed the ABS prescribed limits for concrete with regard to fatigue, serviceability (including water-tightness), and ultimate strength.

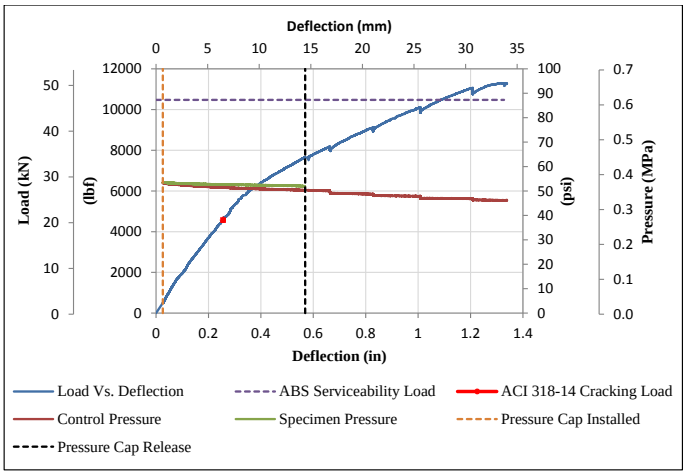

FIGURE 19. FATIGUE B #3 ULTIMATE STRENGTH TEST, MAXIMUM LOAD 11,288 LBF

Based on the results from this testing effort, the following conclusions were made:

- The concrete system considered maintains water-tightness up to ultimate bending strength of the concrete section when loaded in one direction.
- The concrete system considered maintains water-tightness beyond the ABS serviceability loading limit when subjected to flexural loads.
- The ABS serviceability load limit is near the ultimate strength of the specimen when determined from visual inspection of cracks.
- A small loss of 6.7% was recorded in the ultimate bending strength capacity of the section due to the 200 psi (1.38 MPa) fatigue A cycling.
- A small loss of 6.9% was recorded in the ultimate bending strength capacity of the section due to fatigue B cycling which caused cracking on one side of the specimens.
- No loss in water-tightness due to either fatigue regime was observed.
- The two fatigue loading regimes, can be used as conservative fatigue limits when designing concrete for resistance to fatigue due to bending.

This work was reviewed by ABS and served to qualify the design methods for the first concrete floating wind turbine in the U.S. scheduled for grid-connection in 2019.

ACKNOWLEDGMENTS

The authors would like to acknowledge the financial support of the U.S. Department of Energy Grant No. DE-EE0006713, CEED ERDC Grant No. SINIT-13-0018, the state of Maine, and the University of Maine.

NOMENCLATURE

ABS American Bureau of Shipping
FOWT Floating Offshore Wind Turbines
LCOE Levelized Cost of Energy
LNG Liquefied Natural Gas
MW Megawatt
MT Metric Ton
NREL National Renewable Energy Laboratory

REFERENCES

[1] Viselli, A. M., Dagher, H. J., and Goupee, A. J., 2014, "Model Test of a 1:8 Scale Floating Wind Turbine Offshore in the Gulf of Maine," in *Proceedings from the ASME 33rd International Conference on Ocean, Offshore and Artic Engineering*, San Francisco, California, USA.

[2] Viselli, A. M., Dagher, H. J., Goupee, A. J., and Allen, C. K., 2015, "Design and Model Confirmation of the Intermediate Scale VolturnUS Floating Wind Turbine Subjected to its Extreme Design Conditions," *Wind Energy Journal*.

[3] Viselli, A. M., Dagher, H. J., Goupee, A. J., Allen, C. K., and Libby, C., 2015, "VolturnUS 1:8-Successful Completion of 1 1/2 Years of Testing the First Grid-Connected Offshore Wind Turbine in the Americas," in *Proceedings of the 20th Offshore Symposium Sponsored by the Texas Section of SNAME*, Houston, Texas, USA.

[4] Viselli, A. M., Dagher, H. J., Goupee, A. J., and Allen, C. K., 2015, "VolturnUS 1:8: Conclusion of 18-months of Operation of the First Grid-Connected Floating Wind Turbine Prototype in the Americas," in *Proceedings from the ASME 34th International Conference on Ocean, Offshore and Artic Engineering*, St. John's, Newfoundland, Canada.

[5] Viselli, A. M., Dagher, H. J., and Goupee, A. J., 2015, "Model Test of a 1:8-Scale Floating Wind Turbine Offshore in the Gulf of Maine," *Journal of Offshore Mechanics and Artic Engineering*, **137**(4).

[6] Allen, C. K., Goupee, A. J., Viselli, A. M., and Dagher, H. J., 2015, "Validation of Global Performance Numerical Design Tools Used for Design of Floating Offshore Wind Turbines," in *Proceedings from the ASME 34th International Conference on Ocean, Offshore and Artic Engineering*, St. John's, Newfoundland, Canada.

[7] Musial, W. D., and Ram, B., 2010, "Large Scale Offshore Windpower in the United States: Assessment of Opportunities and Barriers. NREL/TP-500-40745," National Renewable Energy Laboratory.

[8] U.S. Department of Energy, 2016, "National Offshore Wind Strategy".

[9] James, R., and Ros, M. C., 2015, "Floating Offshore Wind: Market and Technology Review," Carbon Trust.

[10] LØset, Ø., and Haakonsen, K. O., 1995, "Troll Oil: The first concrete FPS," Offshore Technology Conference OTC-7943-MS.

[11] Snyder, J., 1992, "Heidrun - A Breakthrough for Concrete Technology," *Maritime Reporter and Engineering News*, p. 58, (7).

[12] Moksnes, J., Hoff, G. C., and Fjeld, S., 1994, "Concrete Platforms: History, Technological Breakthroughs, And Future," Offshore Technology Converence OTC-7630-MS.

[13] Yee Precast Design Group, 2017, "Concrete Island Drilling Station (CIDS)," [Online]. Available: http://precastdesign.com/projects/platforms-barges/CIDS_gallery.php#1_CIDS/CIDS_1.jpg.

[14] ACI Committee 357, 2010, "Report on Floating and Float-in Concrete Structures (ACI 357.2R-10)," American Concrete Institute (ACI).

[15] Sofia, M. J., and Homsi, E. H., 1994, "Fabrication and Erection of Precast Concrete Segmental Boxes for Baldwin Bridge," *PCI Journal*, **39**(6), pp. 36-52.

[16] Tepfers, R., 1979, "Tensile Fatigue Strength of Plain Concrete," *ACI Journal*, **76**(8), pp. 919-934.

[17] Oh, B. H., 1986, "Fatigue Analysis of Plain Concrete in Flexure," *Journal of Structural Engineering*, **112**(2), pp. 273-288.

[18] Shi, X. P., Fwa, T. F., and Tan, S. A., 1993, "Flexural Fatigue Strength of Plain Concrete," *ACI Materials Journal*, **90**(5), pp. 435-440.

[19] Arthur, P. D., Earl, J. C., and Hodgkiess, T., 1979, "Fatigue of Reinforced Concrete in Seawater," *Concrete*, pp. 26-31.

[20] El Shahawi, M., and d. Batchelor, B., 1986, "Fatigue of Partially Prestressed Concrete," *Journal of Structural Engineering*, **112**(3), pp. 524-537.

[21] Viselli, A. M., Forristall, F. Z., Pearce, B. R., and Dagher, H. J., 2015, "Estimation of extreme wave and wind design parameters for offshore wind turbines in the Gulf of Maine using a POT method," *Ocean Engineering*, **104**, pp. 649-658.

[22] Martin, H. R., Kimball, R. W, Viselli, A. M., and Goupee, A. J., 2014, "Methodology for Wind/Wave Basin Testing of Floating Offshore Wind Turbines," *Journal of Offshore Mechanics and Arctic Engineering*, **136**(2).

[23] American Bureau of Shipping, 2010, "Guide for Building and Classing Gravity-Based Offshore LNG Terminals".

[24] ACI Committee 318, 2014, "Building Code Requirements for Structural Concrete (ACI 318-14)," American Concrete Institute (ACI).

[25] M. A. Miner, M. A., 1945, "Cumulative damage in fatigue," *Journal of Applied Mechanics*, pp. A159-A164.

[26] DNV, 2012, "DNV-OS-C502 Offshore Concrete Structures," Det Norske Veritas AS.